Reduction and Polymorphic Transformation of B-Nb_2O_5

By **S. Kamal E. Forghany** and **J. Stuart Anderson,*** † Inorganic Chemistry Laboratory, University of Oxford, South Parks Road, Oxford OX1 3QR

The modification B-Nb_2O_5, theoretically the stable polymorph below *ca.* 940 K, undergoes no transformation to the high-temperature stable H-Nb_2O_5 under oxidising conditions, below *ca.* 1 220 K. Reducing conditions facilitate the transformation. At or below 1 020 K, B-Nb_2O_5 is reduced directly to NbO_2, without traversing any intermediate oxides; reaction is topologically controlled by relations between the structures. Under buffered oxygen fugacities, reduction and transformation take place simultaneously at and above *ca.* 1 100 K. Electron microscopy shows that the product is a non-equilibrium intergrowth of H-Nb_2O_5 with structural elements of the lower, mixed-valence, block-structure oxides. A new regular intergrowth structure, $Nb_{43}O_{107}$, has been detected as an extensive ordered domain and this, with an associated extended defect, suggests a mechanism for the formation of Wadsley defects and disordered intergrowths in the reduction of H-Nb_2O_5 at below 1 300 K. The transformation B-Nb_2O_5 ⟶ H-Nb_2O_5 is discussed in terms of alternative reaction paths. Formation of block structures is nucleation-controlled, and appears to be catalysed by platinum.

NIOBIUM PENTAOXIDE forms a remarkably large number of polymorphs, most of which have structures derived from the ReO_3 type, collapsed in different ways by crystallographic shear (c.s.) to form the so-called block structures (*e.g.* the H, N, P, M, and R modifications,[1] and also the forms of Nb_2O_5 produced by oxidising the mixed-valence oxides $Nb_{12}O_{29}$, $Nb_{22}O_{54}$, $Nb_{47}O_{116}$, $Nb_{25}O_{62}$, and $Nb_{53}O_{132}$ at low temperatures [1,2]). The T and TT polymorphs are structurally related to L-Ta_2O_5, and B-Nb_2O_5 has a unique structure, determined by Laves *et al.*[3] It consists (Figure 1) of rutile-like ribbons or sheets of edge-sharing co-ordination octahedra, two octahedra across, joined by vertex sharing, and it can be regarded [4] as derived from the PdF_3 structure,

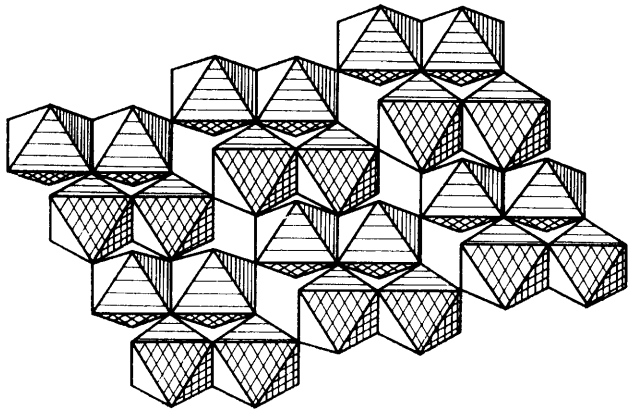

FIGURE 1 Structure of B-Nb_2O_5: rutile-like sheets linked by corner-sharing octahedra

collapsed by crystallographic shear, or from the rutile structure expanded by crystallographic shear. The hexagonal packing of oxygens in this structure cannot be transformed into the cubic packing, found in the structures derived from the ReO_3 type, without a substantial degree of reconstruction and extensive, co-operative atom movements.

Most of the polymorphic structures are undoubtedly metastable. It is probable that N-Nb_2O_5 can be formed only if stabilising defects or substituents are present; electron microscopic studies in our laboratory cast some doubt on the real status of M-Nb_2O_5, even though Mertin *et al.*[5] have reported a crystal structure. The modification H-Nb_2O_5 is the stable form, into which all the other modifications are irreversibly converted at 900—1 000 °C, at ordinary atmospheric pressures. However, Tamura [6] found that both T- and B-Nb_2O_5 are equilibrium phases under high pressures. From his results, the boundaries of the stability fields are given approximately by relations (1) and (2). Extrapolation would indicate that

$$P/\text{kbar}\ (H\text{-}/T\text{-}) = 0.02(T/\text{K}) - 20.5 \quad (1)$$

$$P/\text{kbar}\ (T\text{-}/B\text{-}) = 0.18(T/\text{K}) - 169 \quad (2)$$

B-Nb_2O_5 should be the absolutely stable modification below *ca.* 670 °C, at 1 bar.‡ Except at high temperatures, however, the solid-state transformations are very sluggish and H-Nb_2O_5 is the only operationally stable form.

Temperatures found for the transformation B-Nb_2O_5 ⟶ H-Nb_2O_5 vary to some extent with the experimental conditions. Transformation is necessarily reconstructive and the slow step is probably that of initial nucleation. Reducing conditions facilitate the conversion; B-Nb_2O_5 then transforms at and above 800 °C into H-Nb_2O_5 and its reduction products, the mixed-valence block-structure oxides. In our experiments, the initiation of the relevant processes appeared to be catalysed by platinum. Below 800 °C there was no transformation into block-structure products; instead, reduction took place but followed a different, essentially non-reconstructive course.

EXPERIMENTAL

Well grown crystals of B-Nb_2O_5 were prepared by chemical vapour transport, using $NbCl_5$ as transport agent and a temperature gradient of 750 to 700 °C. The transport ampoules were charged with 0.5 atm of Cl_2, at room temper-

† *Present address*: Edward Davies Chemical Laboratory, University College of Wales, Aberystwyth, Dyfed SY23 1NE.

‡ Throughout this paper: 1 bar = 10^5 Pa; 1 atm = 101 325 Pa; 1 cal = 4.184 J.

ature, to maintain oxidising conditions. Hand-picked colourless crystals were finely ground, to provide a large surface area for the reduction-transformation experiments.

Transformation and reduction experiments were carried out either on a Cahn RG4 microbalance or in a furnace, designed to permit very rapid heating and quenching in a controlled atmosphere.[7] Both were attached to a gas-circulation line, whereby buffer gas mixtures (CO_2–CO and CO_2–H_2) could be passed over the sample at constant pressure, to establish a defined oxygen fugacity.

Products of the transformation–reduction process were characterised by analysis (reoxidation to Nb_2O_5 on the Cahn balance), by *X*-ray diffraction (Guinier camera, Cu-$K_{\alpha 1}$ radiation), and by electron diffraction and high-resolution electron microscopy. The rate of the reduction process and the overall composition change were followed directly by the microbalance; the phases produced, and the relative roles played by reduction and by direct polymorphic transformation, could be deduced from the diffraction evidence.

The ultramicrostructure, the presence of defects, and the extent of ordering in the crystalline products were examined by lattice-imaging electron microscopy. A Siemens 102 electron microscope was used and images were obtained by standard procedures, from the thin (<10 nm) edges of crystalline fragments, at 70–90 nm under focus. Under these conditions, the images furnished by crystals of block structures approximate well to the projected charge-density distribution, and they can be directly interpreted in terms of local structure.

RESULTS

Reduction of B-Nb_2O_5 *at* 750 °C.—Reduction at lower temperatures is essentially non-reconstructive. Samples (50 mg) of *B*-Nb_2O_5 were heated on the microbalance, in CO_2–H_2 mixtures covering oxygen fugacities between 9.84×10^{-20} ($CO_2 : H_2 = 4.67 : 1$) and 1.96×10^{-23} ($CO_2 : H_2 = 0.05 : 1$) in 26 steps. The products were characterised by *X*-ray diffraction, and the results are summarised in Table 1. In a second series of experiments, also at 750 °C,

TABLE 1

Transformation and reduction of *B*-N_2O_5 at 750 °C

Ratio $CO_2 : H_2$	4.67—0.55	0.43—0.13	0.10—0.05
log (p_{O_2}/atm)	−19.01 −20.73	−20.94 −21.90	−22.13 −22.73
Reaction	Nil	slow reduction	rapid reduction
		Reaction accelerating →	

reaction was quenched after reaching progressively higher degrees of reduction, in order to detect any intermediate stages in the reduction process. As shown in Table 2 and Figure 2(*a*) NbO_2 is the sole product of reduction, from the earliest detectable stage, under an oxygen pressure of *ca.* 1.6×10^{-21} atm.

Exactly parallel results were obtained using a CO_2–CO buffer, showing that the results in Table 2 were not invalidated by neglect of any thermomolecular segregation in the CO_2–H_2 mixture. *X*-Ray evidence shows that NbO_2 progressively builds up during reaction, and is the first and only product of reduction of *B*-Nb_2O_5 at 750 °C.

Transformation and Reduction at Higher Temperatures.—*At* 950 °C. Material heated in air for 1 h, in a platinum boat, gave a diffuse diffraction pattern characteristic of the block structures. In particular, the group of lines at $11.8 \leqslant \theta \leqslant 16.6°$, which is critically important for distinguishing the individual block structures, was very diffuse, but compatible with the presence of highly disordered *H*-Nb_2O_5. Direct transformation undoubtedly occurs at 950 °C, but the resulting crystallites of *H*-Nb_2O_5

TABLE 2

Progressive reduction of *B*-Nb_2O_5 at 750 °C

$CO_2 : H_2$	log p_{O_2}	Degree of reduction (%) *	Phases detected by *X*-ray diffraction
1.80	−19.78	nil	*B*-Nb_2O_5
0.60	−20.67	nil	*B*-Nb_2O_5
0.26	−21.34	5	predominantly *B*-Nb_2O_5 + NbO_2
0.16	−21.76	13	predominantly *B*-Nb_2O_5 + NbO_2
0.10	−22.15	36	*B*-Nb_2O_5 + NbO_2
0.05	−22.71	42	*B*-Nb_2O_5 + NbO_2
0.05	−22.71	78	*B*-Nb_2O_5 + predominantly NbO_2

* Fraction of ultimate weight loss, up to the time reduction was interrupted for sampling.

remain very small. Recrystallisation and ordering, following multiple nucleation, are slow processes.

At 900 °C. No transformation could be detected after heating *B*-Nb_2O_5 in air for 10 h.

A series of experiments, carried out in the quench furnace at progressively lower oxygen fugacities [$-17.10 \leqslant \log (p_{O_2}/\text{atm}) \leqslant -17.77$], showed that block-structure products were formed under these conditions, and that the rate of transformation and/or reduction increased as the oxygen fugacity was lowered (Table 3).

Although the blue colour of the products showed that reduction of Nb^V to Nb^{IV} played a part in the process, all the sharp lines in the diffraction pattern (other than those of unchanged *B*-Nb_2O_5) could be accurately indexed in terms of *H*-Nb_2O_5. The diffuse lines could not be unambiguously indexed; microstructural evidence (see below) suggests that they arose from heavily disordered block structures. Under the conditions used, transformation into the *H*-Nb_2O_5 structure accompanies and keeps pace with reduction.

At 880 °C. In a stepwise experiment at 880 °C, a sample (50 mg) showed an initial weight loss of 10 μg h^{-1} at log $p_{O_2} = -16.25$. Reaction slowed down during 5 h, and the

TABLE 3

Reduction and/or transformation of *B*-Nb_2O_5 at 900 °C

$CO_2 : H_2$	log p_{O_2}	*X*-Ray diffraction evidence	
0.21	−17.10	*B*-Nb_2O_5:	predominant
		Product phases:	weak and diffuse pattern
0.18	−17.24	*B*-Nb_2O_5:	predominant
		Product phases:	increased intensity *
0.14	−17.47	*B*-Nb_2O_5:	medium intensity
		Product phases:	medium intensity *
0.11	−17.69	*B*-Nb_2O_5:	present
		Product phases:	predominant *
0.09	−17.77	*B*-Nb_2O_5:	weak
		Product phases:	predominant *

* Both sharp and diffuse lines.

weight eventually remained nearly constant for 12 h. The sample was quenched and a portion removed for *X*-ray analysis. It was then returned, in four steps, to a lower oxygen fugacity, log $p_{O_2} = -18.72$; an *X*-ray sample was withdrawn at each stage. The same sequence, of an initial weight loss, decelerating reaction, and a final nearly con-

stant weight after 11—12 h, was recorded at each stage. The progressive conversion of B-Nb_2O_5 into block-structure products can be traced in Figure 2(*b*).

Visual inspection, at each stage, showed that reduction took place neither uniformly nor at the free upper surface of the powdered sample, but began at the bottom of the layer, where B-Nb_2O_5 was in contact with the platinum bucket.

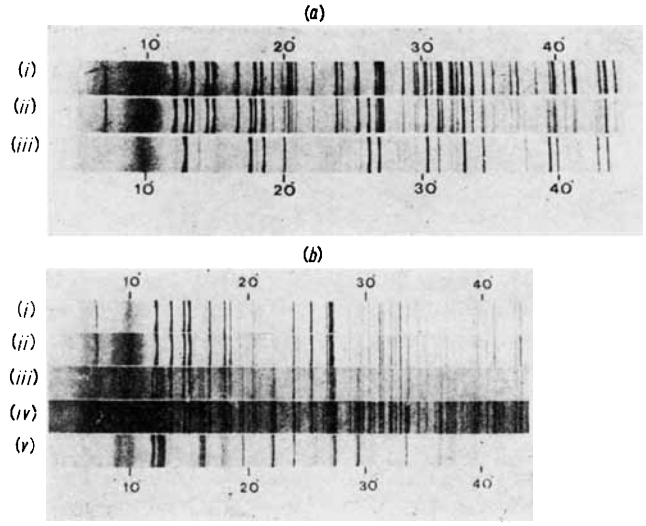

FIGURE 2 Guinier X-ray diffraction patterns of : (*a*)(*i*) B-Nb_2O_5; (*ii*) after 42% reduction at 750 °C, log p_{O_2} −22.7; (*iii*) NbO_2, after complete reduction; (*b*) (*i*) B-Nb_2O_5; (*ii*)—(*v*) progressive conversion to block-structure oxides during transformation under reducing conditions, at 880 °C, log p_{O_2} being lowered in steps from −15.7 to −17.7

Once block-structure products had been nucleated there, the locus of continued reaction was the interface between a layer of converted material and the unchanged B-Nb_2O_5 above it. A deep blue lower layer of transformation products thickened as reaction proceeded, while the upper layer and free surface remained almost white until the last stages of reaction. Nucleation of block structures appeared to be catalysed by platinum (see below).

A separate thermogravimetric experiment, carried out at log p_{O_2} = −17.68, showed that when the sample reached a nearly constant weight its average composition was $NbO_{2.455}$; its diffraction pattern was identical with that shown in Figure 2(*b*)(*v*). Evidence from electron microscopy indicated that any one crystalline particle was substantially uniform in composition, but was not structurally homogeneous. The average composition of different crystalline particles (determined from the micrographs by counting the basic structure elements) could show significant variations; the ' plateau ' composition is only a kinetically determined, fortuitous sample average.

Electron Microscopy of the Transformation and Reduction Products.—Well resolved lattice images were obtained from 15 different crystals. This number probably suffices to give a representative sample of the main microstructural features. Some crystals displayed relatively large areas of well ordered structure, but about two thirds of the areas examined were highly disordered in the (*h*0*l*) projection; their microstructure was a jigsaw of columns with a variety of cross sections and modes of linkage. Image contrast indicative of jogs or disorder along the [010] projection direction was rare, however. The variety of block sizes and, correspondingly, of local stoicheiometry, suggests that transformation and reduction do not proceed by orderly accretion on to a relatively small number of nuclei, but that reconstruction takes place at the reaction interface too rapidly to permit rearrangement and ordering. Elements of different structures, once formed, act as a template for the deposition of further product. As has frequently been observed, one-dimensional ordering, along the [010] axis, is nearly perfect; growth is so propagated as to replicate the underlying template from layer to layer.

On the working assumption that the blocks are substantially free from defects, and the tetrahedral sites ideally occupied, the local composition of any region in a lattice image can be deduced from a count of block dimensions. Table 4 summarises such an analysis of several areas, and

TABLE 4

Block-size analysis and composition of areas in micrographs reproduced

	Figure 3		Figure 5		
Block size	X	Y	Z	Y	X
$(4 \times 3)_1$	5	16.7	0	0	6.7
$(4 \times 3)_2$	40	26.7	48.3	36.1	43.3
$(4 \times 3)_\infty$	5.3	0	5.2	8.4	14.4
$(5 \times 3)_\infty$	21.6	40	25.8	30	15.4
$(3 \times 3)_1$	0	0	1.4	0	7.7
$(3 \times 3)_\infty$	0	3.3	0	0	0
$(4 \times 4)_\infty$	25	13.3	19	25.3	10.6
Other	3.2	0	0	0	1.9
O : Nb (mean)	2.484_6	2.484_4	2.479_0	2.477_0	2.464_9

shows how disordered crystals may be roughly uniform in composition. The high proportion of elements of metastable polymorphs of Nb_2O_5 [N-Nb_2O_5, $(4 \times 4)_\infty$; $Nb_{10}O_{25}$, $(3 \times 3)_1$] is noteworthy; $(4 \times 3)_1$ blocks, contiguous to $(5 \times 3)_\infty$ blocks, constitute elements of the stable H-Nb_2O_5 structure. Units of the $(4 \times 3)_2$ structure ($Nb_{25}O_{62}$) are frequently juxtaposed to elements of the H-Nb_2O_5, or $Nb_{22}O_{54}$, structure, forming microdomains of the intergrowth structures $Nb_{54}O_{132}$ and $Nb_{47}O_{116}$.

Figure 3 shows a lattice image from a disordered crystal (transformed at 850 °C, log p_{O_2} = −19.72). Region Z, although observed largely in relatively thick crystal, can be identified as ordered $Nb_{25}O_{62}$ structure, with occasional Wadsley defects of H-Nb_2O_5 structure. Its composition can be estimated as rather richer in oxygen than $NbO_{2.48}$, in agreement with that of regions X and Y (Table 4). In region Y, at P, rows of the H-Nb_2O_5 and $Nb_{25}O_{62}$ structures alternate almost regularly, to form a domain of $Nb_{53}O_{132}$. Throughout Z and P there is a common orientation of CS planes, suggesting growth from a common template nucleus. In region M (mapped in Figure 4) this common orientation breaks down and passes into a jigsaw arrangement and distribution of block sizes, with substantial elements of both N- and H-Nb_2O_5 structures, but with the composition adjusted to the crystal average by an excess of $(5 \times 3)_\infty$ and $(4 \times 3)_2$ blocks.

A more highly disordered region from a different crystal fragment, obtained under the same oxygen fugacity, is shown in Figure 5. In this the average composition is again the same for regions of different, disordered microstructure. In region X, part of which is mapped in Figure 6, are elements of the N-Nb_2O_5 (N), H-Nb_2O_5 (D), and $Nb_{22}O_{54}$ (Q) structures. The spatial constraints in forming the disordered block structure are accommodated by building in blocks of abnormal dimensions and configuration at

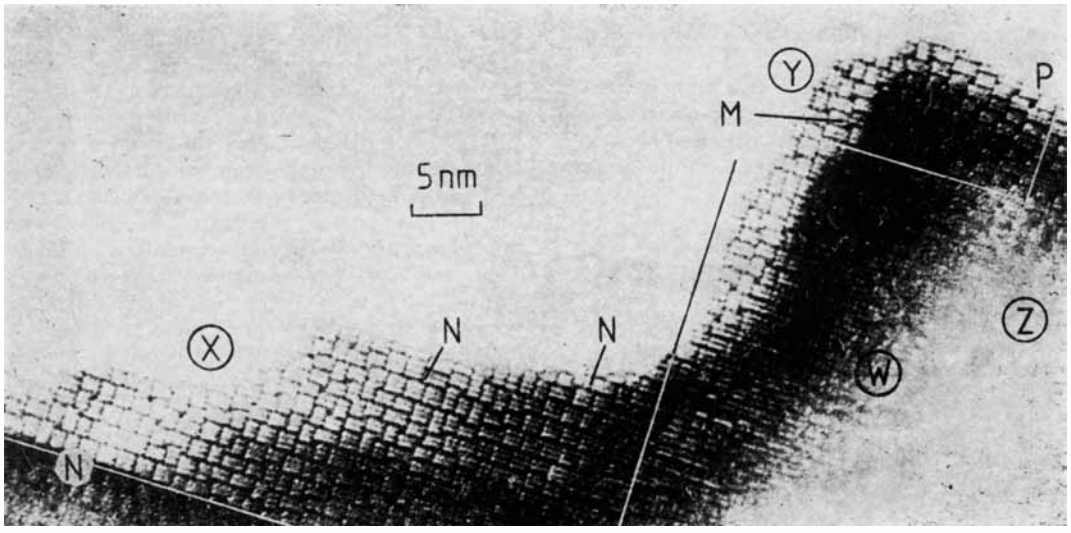

FIGURE 3 High-resolution micrograph of crystal from treatment of B-Nb_2O_5 at 850 °C, log p_{O_2} −19.3. Areas W and X have disordered block arrangements; Z has partially ordered $Nb_{25}O_{62}$ with intergrowths of $Nb_{28}O_{70}$. Elements of the N-Nb_2O_5 structure are shown at N

V, and a line of ' spliced ' blocks, at T, of which the rectangular tunnels (0.56 × 0.28 nm) show up as white contrast streaks. There is evidence from previous work that such ' spliced ' blocks are not infrequently found in materials that have been quenched whilst undergoing re-ordering processes; they may represent frozen-in, transitional configurations.

Also found were small microdomains of regularly ordered intergrowth structures that correspond to no known, stable, intermediate phases. Figure 7 is a micrograph from a crystal treated under the same conditions as that in Figure 3. Over much of the image field, and clearly identifiable on the right, at Y, the structure is that of well ordered H-Nb_2O_5. Two Wadsley defects can be seen: C, lying on $(60\bar{1})_R$ (the subscript R denoting that the orientation is defined with reference to the underlying ReO_3-type substructure), is a

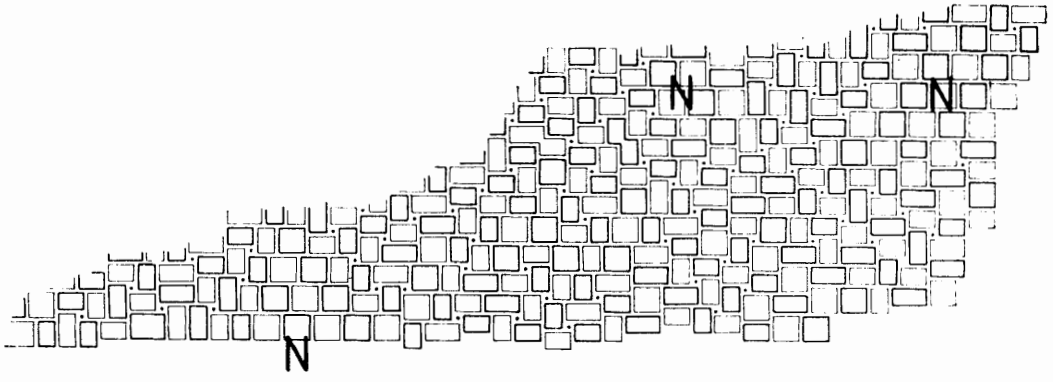

FIGURE 4 Structure map of disordered area X in Figure 3

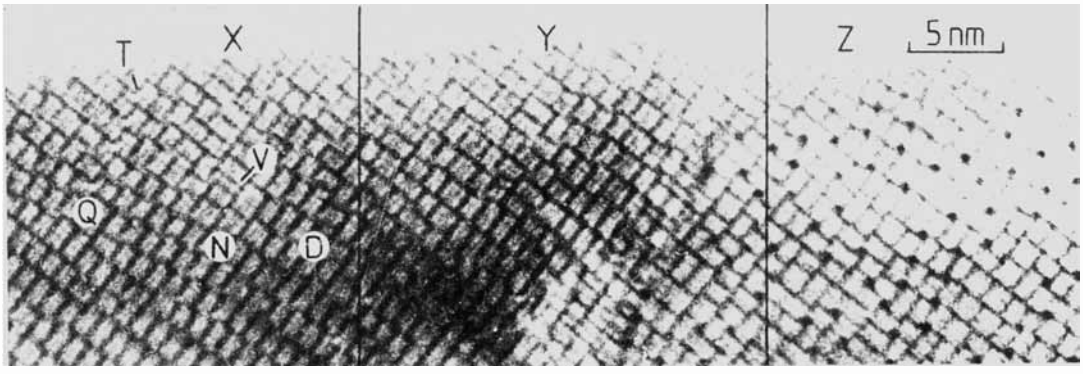

FIGURE 5 High-resolution micrograph of crystal from treatment of B-Nb_2O_5 at 850 °C, log p_{O_2} −19.3. Compositions of disordered areas X, Y, Z are $NbO_{2.465}$, $NbO_{2.477}$, and $NbO_{2.479}$ respectively

single file of the $Nb_{25}O_{62}$ atructure which terminates within the crystal, where it intersects F; F is a stacking error in the H-Nb_2O_5 structure, the insertion of an extra row of $(5 \times 3)_\infty$ blocks. At Z the configuration seen in F recurs regularly,

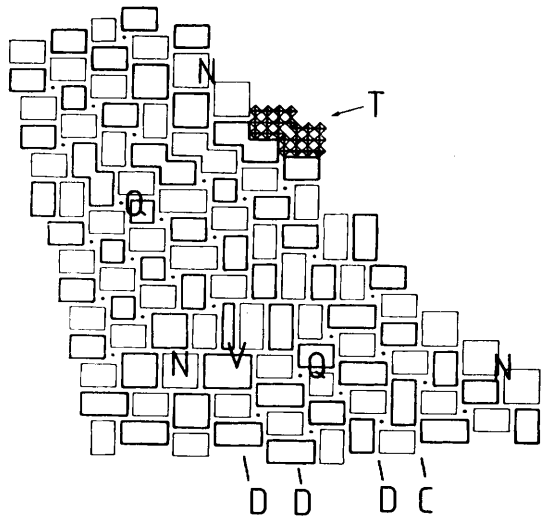

FIGURE 6 Structure map of area X in Figure 5

giving a small domain with the regular alternation $(4 \times 3)_1 + 2(5 \times 3)_\infty$ (see map, Figure 8). The repeating unit of this structure would have a monoclinic cell with the approximate dimensions $a = 2.03$, $b = 0.38$, $c = 6.16$ nm, $\beta = 117°$, and the composition $Nb_{43}O_{107}$. On the left-hand side of Z this microdomain terminates when it intersects a (terminating) domain of $Nb_{53}O_{132}$. An examination of the shifts in atomic positions that relate the H-Nb_2O_5, $Nb_{53}O_{132}$, $Nb_{43}O_{107}$, and $Nb_{25}O_{62}$ structures casts a suggestive light on the mechanism whereby reduction or oxidation processes

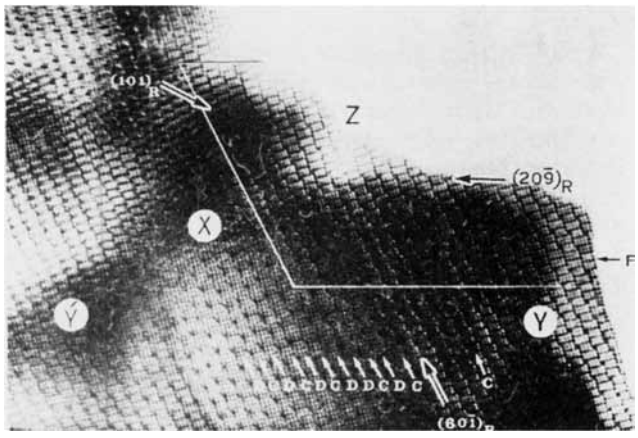

FIGURE 7 High-resolution micrograph of well ordered crystal from treatment of B-Nb_2O_5 at 850 °C, log p_{O_2} −19.3. Region Y: H-Nb_2O_5 structure coherently intergrown (region X) with $Nb_{53}O_{132}$ showing alternating files of $Nb_{28}O_{70}$ (D) and $Nb_{25}O_{62}$ (C). Region Z: new intergrowth structure $Nb_{43}O_{107}$, coherent with $Nb_{28}O_{70}$ and $Nb_{53}O_{132}$. C, F, are Wadsley defects intersecting and terminating within area Z

can take place *within* the block structures, to form coherently intergrown products.

Across the chevron-shaped fault pair C–F two areas of perfect H-Nb_2O_5 structure are mutually displaced. Consider the reduction of H-Nb_2O_5 to $Nb_{25}O_{62}$. The number of niobium atoms in any crystal particle does not change; one oxygen atom has to be eliminated for every two formula units of $Nb_{25}O_{62}$ formed [*i.e.* for every two pairs of $(4 \times 3)_2$ blocks]. The number of files of blocks parallel to $(60\bar{1})_R$ must be increased by *ca.* 12%; a corresponding number of CS interfaces has to be created and there must be a considerable reshuffling of $(60\bar{1})_R$ planes, the composition planes of the coherent intergrowth. However, no long-range atom movements are required to effect these changes. The oxygen sublattice is almost invariant in the original and final structures. No cation need execute a shift of more than the unit diffusion jump of the ReO_3 structure, $\frac{1}{2}a_R$ ⟨110⟩ or $\frac{1}{2}a_R$ ⟨111⟩. Co-operative unit jumps of this kind, across an entire c.s. plane, would advance that c.s.

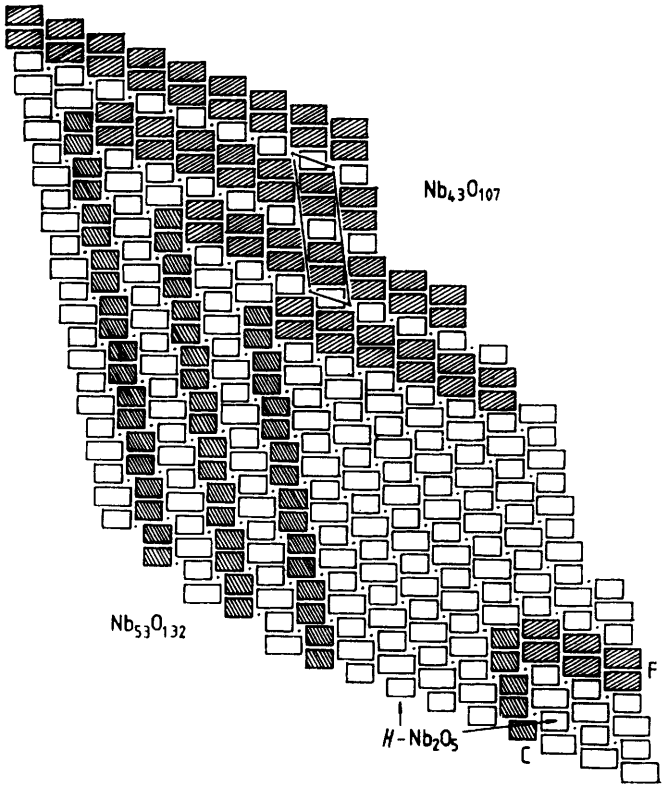

FIGURE 8 Structure map of part of area Z in Figure 7

plane by a_R ⟨100⟩, without change of stoicheiometry, as was postulated by Andersson and Wadsley.[8] This mechanism provides for the reshuffling of c.s. interfaces between files of blocks. Any increase in the number of files of blocks most probably takes place by rearrangement and creation of new c.s. planes at the crystal surface, which is the main locus for the actual abstraction of oxygen atoms during reduction. Any internal process for creating or eliminating c.s. planes necessarily involves dislocations, for which there is no evidence in these particular reactions.

In this context, a possible primary step in the formation of the fault C–F is schematised in Figure 9(*a*). A Wadsley–Andersson (W–A) shift of three cations would convert two $(4 \times 3)_1$ blocks a,c and two $(5 \times 3)_\infty$ blocks b,d into a $(4 \times 3)_2$ pair and a $(5 \times 3)_2$ pair. In itself, this step would be conservative in atoms. However, if one electron, transferred from the reductant, is localised on a cation in

blocks a and c, these become a stable element of $Nb_{25}O_{62}$, but the complementary $(5 \times 3)_2$ pair b,d has the local composition $Nb_{31}O_{78}$; it is hyperstoicheiometric and not a viable entity. By propagating the W–A shift from block to block across successive files, the hyperstoicheiometric configuration would be transferred to the external surface, where oxygen is actually removed in the reduction process, and atoms in the outermost cation and anion rows would be available for the formation of new blocks. In this process [Figure 9(*b*)] a double ribbon of $(5 \times 3)_\infty$ blocks is formed, terminating at the element of $Nb_{25}O_{62}$ structure. Also produced is a stacking fault [two consecutive $(4 \times 3)_1$ blocks] in the H-Nb_2O_5 structure, below this double ribbon. Repetition of the electron-transfer and W–A shift processes, operating on blocks y,z . . . would work this fault downwards and out of the crystal, creating another unit of $Nb_{25}O_{62}$ at each step. The entire file a,c.y . . . is thus ultimately converted into a Wadsley defect of $Nb_{25}O_{62}$ that terminates at the double ribbon of $(5 \times 3)_\infty$ blocks first formed, and perfect, but displaced, H-Nb_2O_5 structure is left between the two intersecting faults. It is easy to verify that this chevron-shaped Wadsley defect pair will be displaced upwards and sideways if the same processes operate on $(4 \times 3)_1$ blocks on the outer side of the chevron.

A plausible mechanism for the reduction process is that reaction is initiated at the surface, involving that minimum number of blocks needed to nucleate a chevron-shaped fault pair like C–F. As reduction proceeds, this fault pair migrates or climbs through the crystal, by co-operative W–A shifts, to form one new element of reduced structure for every electron transferred. In general, the fault pair would climb right across the crystal, to form a lamina of $Nb_{25}O_{62}$ sandwiched between good H-Nb_2O_5 and eliminating the complementary double-ribbon fault. Reductive attack that nucleated isolated chevron faults would produce isolated Wadsley defects or randomly stacked intergrowths. If it initiated the W–A co-operative displacements at each $(4 \times 3)_1$ block along a file of blocks, reaction would generate the ordered $Nb_{53}O_{132}$ structure. In Figure 8 we have not only the significant, isolated chevron fault C–F, but also a domain of $Nb_{53}O_{132}$ terminating within the crystal and necessarily abutting on an ordered sequence of compensating faults which constitute the domain of $Nb_{43}O_{107}$.

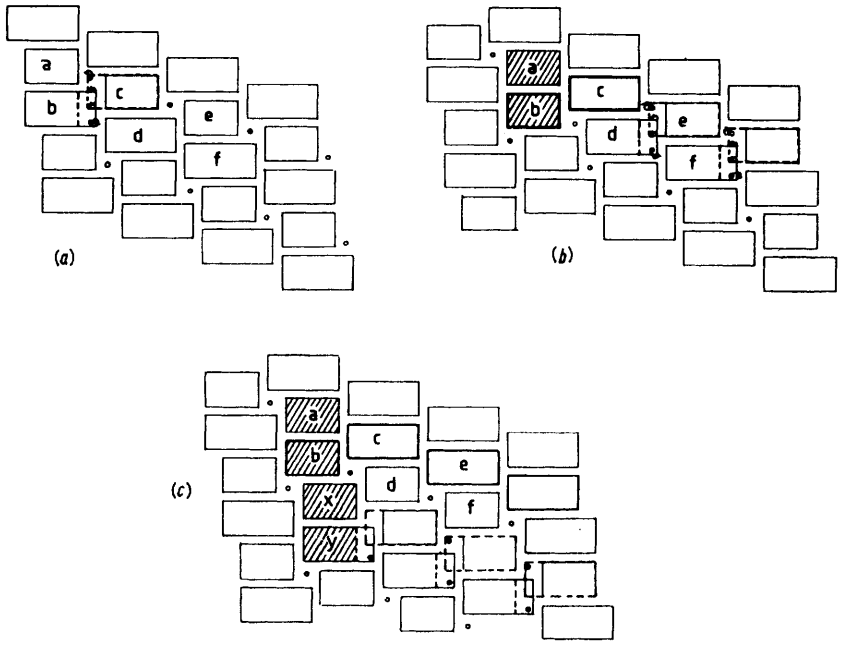

FIGURE 9 Schematic mechanism for the formation of a Wadsley defect of $Nb_{25}O_{62}$ in the reduction of H-Nb_2O_5. The relatively few cation movements needed are indicated

DISCUSSION

Within that temperature range over which it is the thermodynamically stable polymorph, B-Nb_2O_5 is reduced directly to NbO_2. This finding can be compared with Schäfer's observation that NbO_2 is oxidised to B-Nb_2O_5 at relatively low temperatures; because their crystal structures are closely related, only minimally reconstructive reactions are thereby involved. Both the abstraction of oxygen from B-Nb_2O_5 and the insertion of oxygen into the distorted rutile structure of NbO_2 could be visualised as crystallographic shear processes, but experimental evidence is lacking.

At and above 800 °C, the B-Nb_2O_5 structure is certainly unstable with respect to the H-Nb_2O_5 structure, but direct reconstruction is kinetically hindered, probably at the nucleation step. Why reducing conditions should facilitate the conversion can be understood in the light of the ease of reduction of B-Nb_2O_5; this step can furnish a route for the nucleation of block structures and a turnover of material to build into them (Scheme).

Once viable nuclei or small crystallites of H-Nb_2O_5 have already been formed, direct conversion (step I), although kinetically hindered, may take place by a relatively slow particle-to-particle transfer mechanism. Step II, the direct reduction of B-Nb_2O_5 to NbO_2, is

already a moderately rapid process at 750 °C, under conditions more reducing than $CO_2 : CO = 0.53 : 1$; this corresponds to a free-energy change of *ca.* 95 kcal for reaction (3). The free energies of formation of NbO_2

$$2\ B\text{-}Nb_2O_5 \longrightarrow 4\ NbO_2 + O_2 \qquad (3)$$

and Nb_2O_5 (presumably *H*-, but not specified) lead to a considerably larger free energy of reduction of *H*-Nb_2O_5, but may well need revision. The direct reduction of *B*-Nb_2O_5 observed at 750 °C must undoubtedly

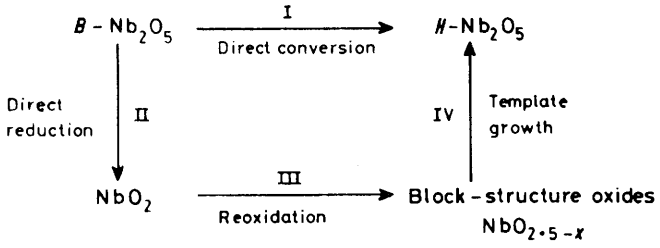

SCHEME

take place, and faster, at 800—900 °C and the range of oxygen fugacities employed in our experiments.

In the temperature range where *H*-Nb_2O_5 is the stable form, there is direct evidence about the thermodynamics of reduction.[9-12] This modification is reduced through a succession of block structures and, because these can intergrow coherently with *H*-Nb_2O_5 and with each other, reduction at 800—1 000 °C simulates the behaviour of a bivariant system. Reaction does not proceed beyond the stage of $Nb_{12}O_{29}$ at an oxygen fugacity of 6.3×10^{-16} atm at 1 020 °C. Under the conditions summarised in Table 3, the expected composition of the pseudo-equilibrium product would be around $NbO_{2.495}$ to $NbO_{2.498}$, within the composition range of the substoicheiometric *H*-Nb_2O_5 structure as found by Gruehn.[13] Hence, if NbO_2 were formed as a transient, direct product of step II, it would be unstable towards oxidation by the ambient gas buffer, and would be converted first into $Nb_{12}O_{29}$ and thence upwards through the succession of block structures (step III). The observed products could arise in this way, as well as by direct transformation followed by reduction. It is unlikely that equilibrium could be preserved during these processes, and the formation of crystals with inhomogeneous structure and composition can be understood. If nucleation is the limiting process in step I the limitation is circumvented once template crystals have been formed (step IV) by the indirect route. Interfacial transfer processes would then determine the relative importance of the direct and indirect modes of transformation.

Platinum appeared to catalyse the formation of suitable template nuclei in the bottom surface of the samples. Since the microbalance bucket had been in long use for similar work, its surface might have been covered by an oxide film of suitable structure (*e.g.* in which octahedrally co-ordinated platinum was already built into some block structure, such as $Pt^{IV}_2Nb_{10}O_{29}$). This explanation is probably ruled out since there was no oxygen uptake or detectable formation of any new phase when an intimate mixture of Nb_2O_5 with finely divided platinum was heated in air. The CO_2–CO and CO_2–H_2 buffers showed identical effects, so that reduction by dissociatively adsorbed hydrogen is unlikely. Some remarkable findings by Moodie and Warble [14] may be relevant. They observed, in the electron microscope, that perfect crystals of the highly refractory MgO (m.p. 2 800 °C) ' dissolved ' by surface migration at 1 000 °C in contact with palladium (m.p. 1 549 °C). This suggests an unexpectedly high mobility at a chemically inert metal–metal oxide interface. If the effect is general (it has become the basis of metal-to-ceramic bonding technologies) it could provide a route for the continuous transfer of material from an unstable to a stable polymorphic oxide, across the platinum surface. No sure explanation can be advanced, but we have repeatedly found the same enhancement of reactivity at the oxide–platinum interface during the preparation of titanium–niobium block-structure oxides.

The authors thank the S.R.C. for support. S. K. E. F. also thanks the Ministry of Science and Higher Education of Iran, and the British Council.

[0/288 *Received*, 19*th February*, 1980]

REFERENCES

[1] H. Schafer, R. Gruehn, and P. Schulte, *Angew. Chem. Internat. Edn.*, 1966, **5**, 40.
[2] H. Hibst and R. Gruehn, *Z. anorg. Chem.*, 1978, **442**, 49.
[3] F. Laves, W. Petter, and H. Wulf, *Naturwiss.*, 1964, **51**, 633.
[4] S. Andersson and J. Galy, *J. Solid State Chem.*, 1970, **1**, 576.
[5] W. Mertin, S. Andersson, and R. Gruehn, *J. Solid State Chem.*, 1970, **1**, 419.
[6] S. Tamura, *J. Mater. Sci.*, 1972, **7**, 298.
[7] S. K. E. Forghany, D. Phil. Thesis, Oxford, 1977.
[8] S. Andersson and A. D. Wadsley, *Nature*, 1966, **211**, 581.
[9] K. M. Nimmo and J. S. Anderson, *J.C.S. Dalton*, 1972, 2328.
[10] R. N. Blumenthal, J. B. Moser, and D. H. Whitmore, *J. Amer. Ceram. Soc.*, 1965, **48**, 620.
[11] H. Schafer, D. Bergner, and R. Gruehn, *Z. anorg. Chem.*, 1969, **365**, 31.
[12] S. Kimura, *J. Solid State Chem.*, 1973, **6**, 438.
[13] R. Gruehn, ' Solid State Chemistry,' N.B.S. Special Publication 364, 1972, p. 63.
[14] A. F. Moodie and C. E. Warble, *Phil. Mag.*, 1977, **35**, 201.